BULLETIN OF THE POLISH ACADEMY OF SCIENCES
TECHNICAL SCIENCES, Vol. 72(4), 2024, Article number: e150329
DOI: 10.24425/bpasts.2024.150329

Multi-unmanned aerial vehicle odor source location based on improved artificial fish swarm algorithm

Tao DING[1]*, Wenhan ZHONG[2], and Yufeng CAI[1]

[1] China Jiliang University, Hangzhou, China
[2] Zhejiang Light Industrial Products Inspection and Research Institute, Hangzhou, China

Abstract. Odor source location technology has important application value in environmental monitoring, safety emergency and search and rescue operations. For example, it can be used in post-disaster search and rescue, detection of hazardous gas leakage, and fire source detection. Existing odor source location methods have problems such as low search efficiency, inability to adapt to complex environments, and inaccurate odor source location. In this study, based on unmanned aerial vehicle technology and using swarm intelligence optimization algorithm, an improved artificial fish swarm algorithm (IAFSA) is proposed by combining curiosity in psychology on the basis of retaining the good optimization performance of the artificial fish swarm algorithm. The algorithm quantifies the curiosity of artificial fish searching high-concentration areas through a model, dynamically adjusts the artificial fish field of vision and step length with the calculated curiosity factor, and avoids the oscillation phenomenon in the later stage of the algorithm. Simulation results show that the IAFSA has a higher success rate and smaller location error. Finally, odor source location experiments were carried out in an indoor physical environment, the feasibility of the odor source location method proposed in this study is verified in actual scenarios.

Keywords: odor source location; artificial fish swarm algorithm; unmanned aerial vehicle; active olfaction.

1. INTRODUCTION

Odor source location technology is a technique used to determine the location of a gas leak or odor source. With this technology, it is possible to track and locate odor sources within a spatial range, enabling rapid response and management of issues such as hazardous gas leaks, air quality problems, and environmental monitoring. Traditionally, odor source location mainly relies on biological olfaction, which has significant limitations and instability. To address this issue, scientists have begun researching and developing odor source location methods based on sensor and data processing technologies to accurately detect and locate odor sources. With the continuous advancement of sensor technology and data processing algorithms, odor source location technology has made significant improvements. Modern odor source location technology uses various gas sensors to perceive the concentration of the target gas, and collects relevant environmental parameters such as wind direction and speed. These data are input into algorithms to infer the location of the odor source through model calculation.

In odor source location technology, common methods include biological detection [1], fixed monitoring network [2, 3] and active location [4–7]. Biological detection method means that full-time personnel bring professional equipment to the scene of the accident to search, or use professionally trained creatures to locate the source of the scene, this method has a long training period, low efficiency, and high risk. The fixed monitoring network method refers to the use of a large number of sensors to form a fixed monitoring network, and the odor source is located by monitoring the changes in the gas concentration value of each sensor node in the network. This method needs to deploy a monitoring network in the fixed area in advance when locating the odor source, and the monitoring range is limited by the cost. The active location method is an approach to detect, track, and locate odor sources by employing mobile robots equipped with sensor devices. This method simulates the olfactory location ability of certain animals, such as mosquitoes [8] and male moths [9], which can perform behaviors such as foraging, mating, and repelling predators by tracking the direction and location of odor sources. Compared with the biological detection method and the fixed monitoring network method, the active location method has great advantages in location accuracy, real-time capability, computational efficiency, adaptability and scalability.

Classified according to the number of robots, the current active odor source location methods include single-robot odor source location method and multi-robot odor source location method. Single-robot odor source location methods mainly include chemical tropism, wind tropism, information tropism, visual assistance, model and estimation based methods, etc. The existing achievements include E. coli algorithm [10], Zigzag algorithm [11], plume center upwind algorithm [12], information trend algorithm [13], adaptive mission planner (AMP) algorithm [14], bi-modal search algorithm, Kernel DM+V algorithm [15], etc. The advantages of the single-robot odor source

*e-mail: dingtao@cjlu.edu.cn

Manuscript submitted 2023-12-11, revised 2024-03-30, initially accepted for publication 2024-04-22, published in July 2024.

location method are low cost and easy implementation, but its small search range and weak robustness make it difficult to apply to practical problems. Compared with the single-robot odor source location method, the multi-robot odor source location method needs to rely on the cooperation and information sharing between multiple robots, and related methods include swarm intelligence based method, formation based method, evolution based method and so on. Existing achievements include pollution-driven UAV control (PdUC) algorithm [16], explorative particle swarm optimization (EPSO) algorithm [17], improved ant colony optimization (IACO) algorithm [18], flux trend algorithm [19, 20], evolutionary gradient search algorithm [21], etc. The multi-robot odor source location method has the characteristics of large search range and strong robustness. The search ability, perception ability and anti-interference ability of multi-robot are much higher than that of single-robot.

In the existing achievements, most of the research is to use ground mobile robots to find the odor source, but they are easily limited by complex terrain environments, including obstacles, slopes, stairs, etc. The more complex the terrain environment is, the more factors the robot considers when moving, the more difficult the path planning is, and the efficiency of odor source location will also be reduced. Unmanned aerial vehicle (UAV) has the ability to move in the vertical direction, and flying in the air can avoid the influence of most terrain environments. Compared with ground mobile robots, UAV is more competent to locate odor source in complex terrain environment.

Artificial fish swarm algorithm (AFSA) [22] is mainly inspired by the predatory prey behavior of fish in nature. In nature, the location with the largest number of fish in a certain water environment is often the place with the most food in the water. The fish will spontaneously gather towards the food-rich location. At the same time, the larger the swarm, the more companions will be attracted. The algorithm imitates the biological characteristics of fish when searching for food, including foraging behavior, random behavior, flocking behavior and tail-chasing behavior. Through the imitation of these behaviors, it can perceive the information in the area to be searched, so as to realize optimization.

The odor source location problem of harmful gases is closely related to human life and property safety. As a swarm intelligence algorithm with high search efficiency and strong global search capability, AFSA can significantly reduce the computational cost of odor source location if applied in this field. However, the AFSA itself is susceptible to parameter influence and prone to oscillation in the later stage of the algorithm. To address this issue, based on UAV technology and AFSA, this study introduces curiosity in psychology and proposes a multi-UAV odor source location method based on improved artificial fish swarm algorithm (IAFSA). This method quantifies the curiosity of artificial fish in searching high-concentration areas through a model. By dynamically adjusting the field of vision and step length of the artificial fish based on the calculated curiosity factor, it effectively avoids the oscillation phenomenon in the later stage of the algorithm. Moreover, this approach can maintain a high success rate and a small location error in the odor source location task.

2. IMPROVED ARTIFICIAL FISH SWARM ALGORITHM BASED ON CURIOSITY

2.1. Traditional artificial fish swarm algorithm

2.1.1. Structure model of artificial fish

The optimization idea of the AFSA is bottom-up. First, the individual in the fish swarm is abstracted to construct a structure model of the artificial fish, and then the individual is expanded to the group, and obtained global optimal result from the free interaction between the groups. The structure model of the artificial fish is shown in Fig. 1.

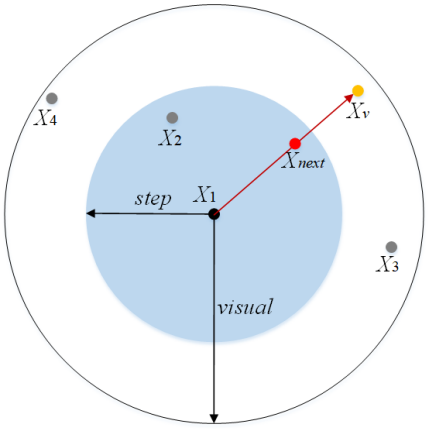

Fig. 1. Artificial fish structure model

The visual field of the artificial fish is *visual*, representing the maximum perception distance of the artificial fish in the search area; *step* is the step length of the artificial fish, representing the maximum distance the artificial fish moves each time; X_1 represents the current position of an artificial fish, X_2, X_3 and X_4 represent the positions of the artificial fish partners; X_v represents the position selected by the artificial fish in the visual field. When the food concentration at the position of X_v is greater than the food concentration at the position of X_1, the artificial fish swims in the direction of X_v and reaches the position of X_{next}, otherwise, the artificial fish will continue to perceive the food concentration information of other positions in the field of vision. With the increase in perception times, the artificial fish will have a more comprehensive cognition of the information in the field of vision.

2.1.2. Basic behaviors of artificial fish

Artificial fish has four basic behaviors, random behavior, foraging behavior, clustering behavior and tail-chasing behavior. The artificial fish will evaluate according to its own environment and choose the best behavior for its next state. The specific behaviors are described as follows:

Random behavior is a supplementary behavior of foraging behavior. The implementation is relatively simple, that is, randomly select a direction to move in the field of vision. The expression is as follows:

$$X_{\text{next}} = X_i + step \cdot Rand. \tag{1}$$

In equation (1), X_i represents the current position of artificial fish i; X_{next} represents the moved position of artificial fish i; *step* represents the maximum moving step length of artificial fish; *Rand* represents a random number in the interval $[0, 1]$.

The foraging behavior simulates the behavior of fish shoals to obtain the food they need for survival in the natural environment. The artificial fish selects the moving direction by sensing the food concentration information in the field of vision, and gradually approaches the food source. The expression is as follows:

$$X_j = X_i + visual \cdot Rand, \tag{2}$$

$$X_{\text{next}} = X_i + \frac{X_j - X_i}{\|X_j - X_i\|} \cdot step \cdot Rand, \tag{3}$$

$$X_{\text{next}} = X_i + step \cdot Rand. \tag{4}$$

In the equations, X_j represents the randomly selected position of the artificial fish i in the field of vision; *visual* represents the field of vision of the artificial fish.

In the foraging behavior, the artificial fish i randomly selects a position X_j within the visual field, obtains the food concentration Y_j at the position X_j, and compares it with the food concentration Y_i at the position X_i, when Y_j is greater than Y_i, the artificial fish will move in the direction of the position X_j, and the position information of the artificial fish is updated according to equation (3). Otherwise, the artificial fish continues to search within the field of vision. When the search reaches *try_number* times, the position with higher food concentration is still not found. The artificial fish will perform random behavior, and the position information on the artificial fish is updated according to equation (4).

In nature, clustering is a common behavior of fish. Due to the needs of hunting food and defending against natural enemies, fish tend to spontaneously form clusters. The clustering behavior in the AFSA imitates this habit of fish. The expression of clustering behavior is as follows:

$$X_{\text{next}} = X_i + \frac{X_c - X_i}{\|X_c - X_i\|} \cdot step \cdot Rand. \tag{5}$$

In equation (5), X_c represents the center position of the fish swarm within the field of vision of the artificial fish i.

When the artificial fish performs clustering behavior, it will first determine the number of partners N in the field of vision and the center position X_c of the fish swarm, and then judge whether the center of the fish swarm meets the two conditions of high food concentration and not overcrowded. When the value of Y_c/N is greater than $\delta \cdot Y_i$ (δ is the crowding factor), it means that the condition is satisfied, the artificial fish moves towards the center position X_c of the fish swarm, and the position information of the artificial fish is updated according to equation (5), otherwise the artificial fish executes foraging behavior.

The tail-chasing behavior is the behavior that the fish learns from the optimal individual in the population, which means that the artificial fish moves towards the position where the food concentration is the highest among the partners. The expression of the tail-chasing behavior is as follows:

$$X_{\text{next}} = X_i + \frac{X_b - X_i}{\|X_b - X_i\|} \cdot step \cdot Rand. \tag{6}$$

In equation (6), X_b represents the position with the largest food concentration in the positions of the partners within the visual field of artificial fish i.

When the artificial fish performs tail-chasing behavior, it first determines the position X_b of the optimal partner in the field of vision and the food concentration Y_b. When the value of Y_b/N is greater than $\delta \cdot Y_i$, it means that the food concentration at X_b is high and not overcrowded, the artificial fish moves towards the X_b direction, the position information of the artificial fish is updated according to equation (6), otherwise the artificial fish performs foraging behavior.

2.1.3. Existing problems

AFSA is an algorithm with high optimization efficiency and strong global search ability, which is usually used to deal with complex function optimization problems. In this study, the AFSA is introduced into the odor source location problem, and still retains many advantages in numerical solutions. When using the AFSA to locate the odor source, multiple artificial fish can be used to search in parallel, which improves the search efficiency. In addition, the odor source location result is not affected by the initial position of the artificial fish, so the initial position of the artificial fish can be set randomly. However, the AFSA still has its shortcomings. Although the AFSA adopts random field of vision and step length, the value ranges of them are fixed, and the maximum field of vision and step length are fixed values. This has an impact on the locating effect of odor source.

Figure 2a is the traceability route map when setting large field of vision and step length. It can be seen from the figure that in the later stage of the odor source location task, the artificial fish are close to the odor source, but the field of vision and step length of the artificial fish are still random in a large range. Therefore, the phenomenon of oscillation occurs. The artificial fish moves back and forth in the area close to the odor source, and it is difficult to accurately locate the odor source. Figure 2b is the change curve in the maximum concentration monitored during the odor source location process. The figure shows the change of the maximum concentration value searched by the artificial fish after each iteration. The wide field of vision and step length are conducive to improving the efficiency of the traceability task in the early stage, and can approach the high-concentration area in a short period of time, but the odor source cannot be accurately located in the later stage.

When setting small field of vision and step length, the artificial fish can search for the odor source meticulously and accurately, but to a certain extent, it increases the time of the odor source location task and reduces the efficiency. In addition, it is also easy to cause the artificial fish to fall into a local peak area with a large range. Figure 3 shows the moving routes of the artificial fish when searching for the odor source with small field of vision and step length, the five artificial fish all fall into the local peak areas and can not jump out of the areas after many attempts.

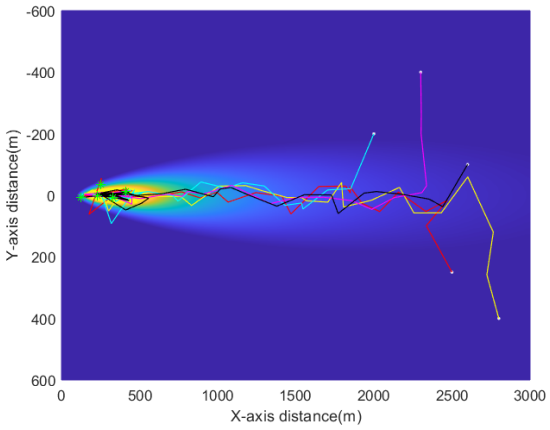

(a) Traceability route map

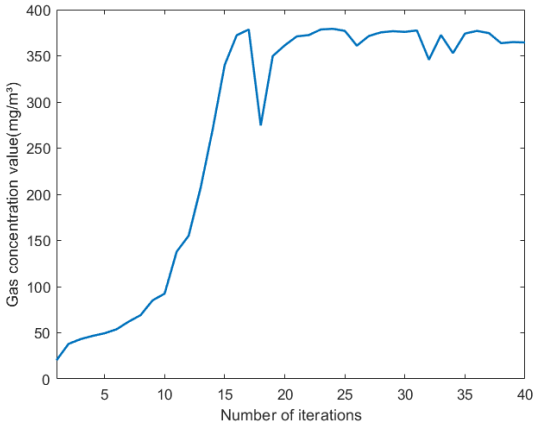

(b) Gas concentration change curve

Fig. 2. Oscillation phenomenon

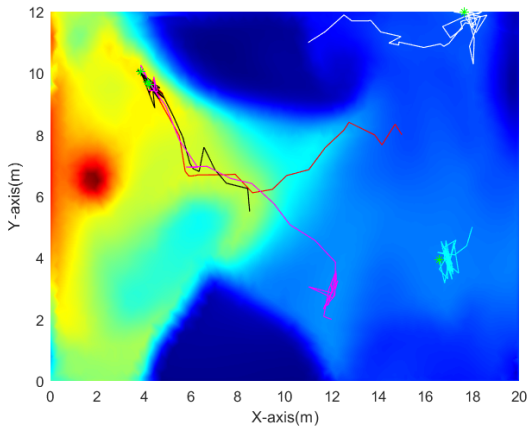

Fig. 3. Artificial fish fall into local peak areas

2.2. Improved artificial fish swarm algorithm based on curiosity

Aiming at the problems existing in the application of AFSA to odor source location, this study proposes an AFSA incorporating curiosity. Curiosity is a psychological concept that expresses the psychological tendency of humans or other creatures to encounter novel things or enter a new environment. Curiosity is also the key motivation for individuals to conduct exploratory behaviors such as searching, investigating and learning. Inspired by this, this study based on the AFSA to construct the artificial fish with curiosity. The artificial fish search time, the number of partners in the field of vision and the food concentration value are used as indicators to measure the artificial fish curiosity, and dynamically adjusts the field of vision and step length of the artificial fish with the calculated curiosity factor to avoid the algorithm defects caused by the fixed value of the maximum field of vision and step length. Artificial fish with strong curiosity have a stronger desire to search for areas with higher food concentration, and their search ranges are larger. On the other hand, artificial fish with weak curiosity have a lower desire to search for areas with higher food concentration, prefer to stay in familiar areas, so their search ranges are smaller.

The artificial fish search time, the number of partners in the field of vision, and the food concentration are the indicators that affect the artificial fish curiosity. The curiosity factor of the artificial fish can be calculated from these three parameters. The value range of the curiosity factor is the interval [0, 1], and its value represents the curiosity of the artificial fish. The larger the value, the stronger the curiosity. Finally, the visual field and step length of the artificial fish are dynamically adjusted by the curiosity factor.

Equations for updating the visual field and step length of artificial fish:

$$step = step \times \alpha, \tag{7}$$

$$visual = visual \times \alpha. \tag{8}$$

In the equations, *step* is the step length; *visual* is the field of vision; α is the curiosity factor of artificial fish.

Equations for calculating the curiosity factor of artificial fish:

$$\alpha = 0.5 \times \left(1 - \frac{iter}{\max\_iter}\right)^{\frac{1}{4}} + 0.25 \times \frac{N}{N_{\max} - 1} + 0.25 \times \left(\frac{Y_{\max} - Y_i}{Y_{\max} - Y_{\min}}\right)^2. \tag{9}$$

In equation (9), *iter* is the number of operation iterations; *max_iter* is the maximum number of iterations; N is the number of partners in the field of vision; $N_{\max}$ is the total number of artificial fish; $Y_{\max}$ is the maximum concentration value found in the fish swarm; $Y_{\min}$ is the minimum concentration value found in the fish swarm; Y_i is the concentration value at the current position of artificial fish i.

The iteration times *iter* can represent the search time of the artificial fish. The larger the *iter*, the longer the artificial fish will search for food. A long search time will cause the artificial fish to be tired. The more tired the artificial fish are, the more they want to stay where they are, and the curiosity to search for areas with higher food concentration will be reduced; when the number N of artificial fish in the field of vision is larger, it means that the current area is being searched by multiple artificial fish, so the unknown information in the current area is gradually decreasing, and it is an important factor affecting curiosity. In nature, people

and other animals usually have great curiosity about unknown and novel things. Therefore, the larger the number N of artificial fish in the field of vision, the stronger the curiosity of artificial fish to search the unknown area outside the current area; $Y_{\max}$ represents the food concentration information obtained by the optimal artificial fish in the population, and Y_i is the food concentration at the current location of artificial fish i. When the difference between artificial fish i and the optimal artificial fish in the population is greater, the artificial fish i is more curious to search for areas with higher food concentration.

Figure 4 is the numerical change curve of the curiosity factor α under the control of a single parameter change, where, the value of iteration number *iter* is an integer in the interval $[0, \max\_iter]$; the value of the number N of partners in the field of vision is an integer in the interval $[0, N_{\max}-1]$; the concentration value Y_i of the current location point is in the interval $[Y_{\min}, Y_{\max}]$. When the value of parameter N is 0, the value of parameter Y_i is $Y_{\max}$, the value of parameter *iter* increases from 0 to $\max\_iter$, the value of $iter/\max\_iter$ will increase from 0 to 1, and the value of curiosity factor α will decrease from 0.5 to 0, the curiosity factor α will decrease with the increase of iteration number *iter*, and the larger the iteration number *iter*, the faster the curiosity factor α decreases; when the value of parameter *iter* is 0, the value of parameter Y_i is $Y_{\max}$, and the value of parameter N increases from 0 to $N_{\max}-1$, the value of $N/(N_{\max}-1)$ will increase from 0 to 1, and the value of the curiosity factor α will increase from 0 to 0.25, the curiosity factor α will increase with the increase of the number N of partners in the field of vision; when the value of parameter *iter* is 0, the value of parameter N is 0, and the value of parameter Y_i increases from $Y_{\min}$ to $Y_{\max}$, the value of $(Y_{\max}-Y_i)/(Y_{\max}-Y_{\min})$ will decrease from 1 to 0, the value of curiosity factor α will decrease from 0.25 to 0, and the value of curiosity factor α will decrease with the increase of the concentration value Y_i of the current location point.

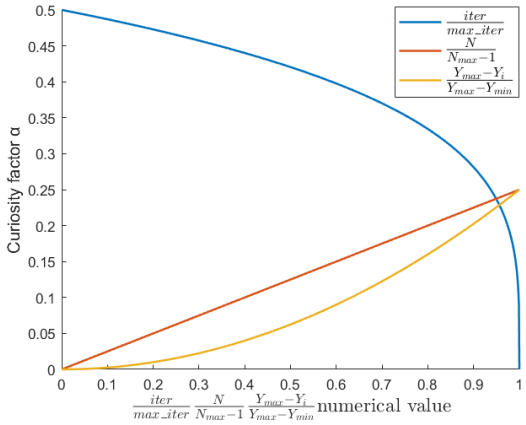

Fig. 4. Curiosity factor α numerical variation curve

In the IAFSA, larger field of vision and step length can be set at the beginning, so as to improve the efficiency of artificial fish to search for the odor source, and in the later stage of the odor source location task, the field of vision and step length of the artificial fish can be significantly reduced by the regulation of curiosity factor to avoid the occurrence of oscillation. When the artificial fish falls into the local optimal solution, the field of vision and step length can also be appropriately increased by the regulation of curiosity factor, so as to improve the probability of the artificial fish jumping out of the local high concentration area.

2.3. The procedural steps of the algorithm

The flow of AFSA incorporating curiosity is shown in Fig. 5.

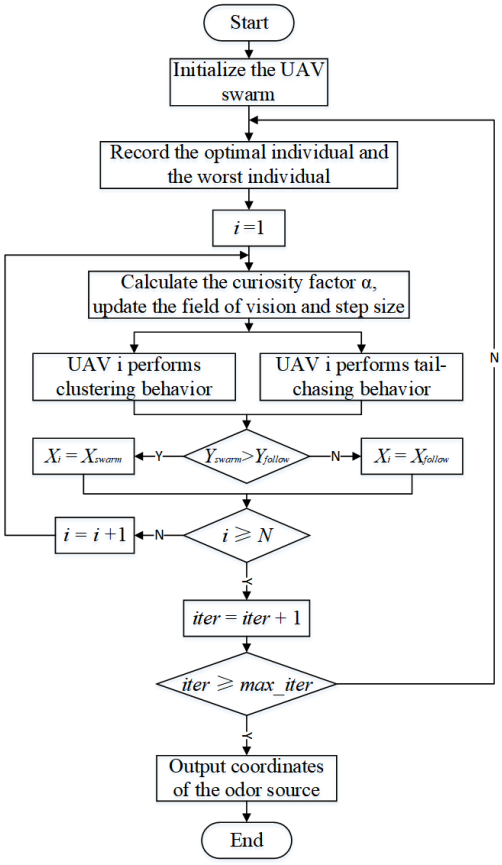

Fig. 5. Flow chart of AFSA incorporating curiosity

The main steps of the AFSA incorporating curiosity are as follows:

Step 1: Initialize the UAV swarm, including setting parameters such as the initial position of the UAVs, the congestion degree δ and the maximum search times *try_number*;

Step 2: Obtain the odor concentration at the location of each UAV, and record the optimal individual and the worst individual;

Step 3: Calculate the curiosity factor of the UAV according to equation (9), and update the field of vision and step length of the UAV according to equation (7) and equation (8);

Step 4: Evaluate the operation status of the UAV, and obtain the position information X_{swarm}, X_{follow} and the odor concentration Y_{swarm}, Y_{follow} after the UAV performs clustering behavior and tail-chasing behavior;

Step 5: Select the behavior to be performed by the artificial fish based on the odor concentration Y_{swarm} and Y_{follow}, and update its position information;

Step 6: Determine whether the number of iterations of the algorithm has reached the upper limit. If not, execute the step 2. If yes, output coordinates of the odor source.

3. SIMULATION EXPERIMENT

3.1. Simulation experiment environment

In this study, the ANSYS Workbench software and computational fluid dynamics (CFD) model [23] were used to build the indoor diffusion simulation experiment environment of smoke plume, which is called CFD simulation concentration field for short. Figure 6 shows the gas concentration distribution on the $Z = 2.5$ m plane in the simulation concentration field. The gas is distributed on a plane with a length of 20 m and a width of 12 m. The coordinates of the odor source are (2, 6.5), and the maximum gas concentration is 16.63 mg/m^3.

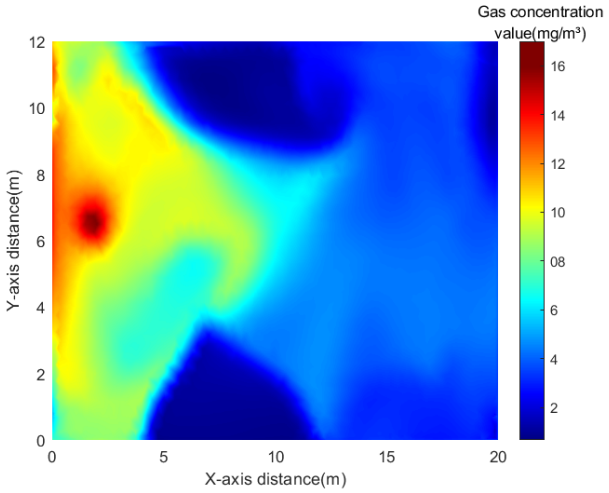

Fig. 6. CFD simulation concentration field

3.2. Performance evaluation index

In this study, the success rate, location error and operation time are selected to evaluate the performance of the multi-UAV odor source location method based on the IAFSA. The success rate refers to the ratio of the number of times the UAV successfully locates the odor source to the total number of experiments in a group of experiments; the location error refers to the distance between the odor source position located by the UAV and the actual odor source position in the simulation experiment, which means the accuracy of locating the odor source; the operation time refers to the average operation time of the simulation experiment that successfully locates the odor source.

3.3. Results and analysis

3.3.1. Influence of the number of UAV on odor source location

Setting up different numbers of UAVs for experiments in the CFD simulation concentration field and controlling the same initial positions of the same number of UAVs. Each group of simulation experiments was conducted 200 times, and the performance of the odor source location method proposed in this study was analyzed through the experimental results. The results of the simulation experiment are shown in Fig. 7.

Figure 7a shows the change curve of the success rate of the simulation experiment results. It can be seen from the figure that when the number of UAV is 1, the success rate of locating the odor source using the three algorithms is similar, and the

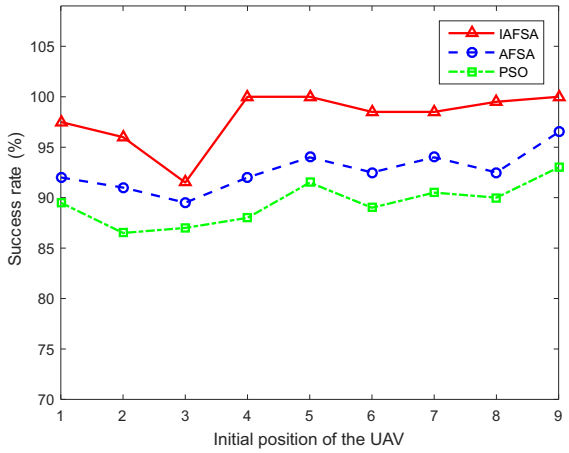

(a) Success rate

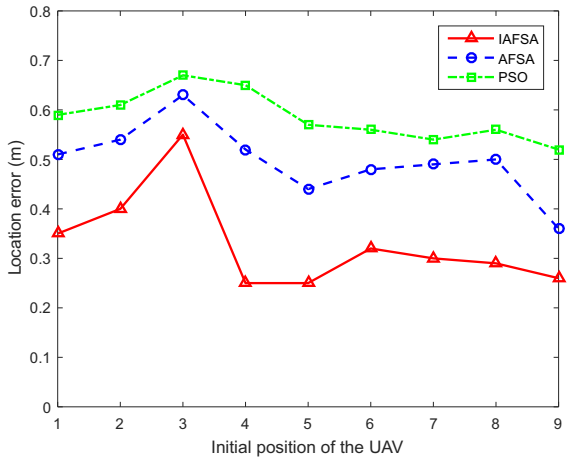

(b) Location error

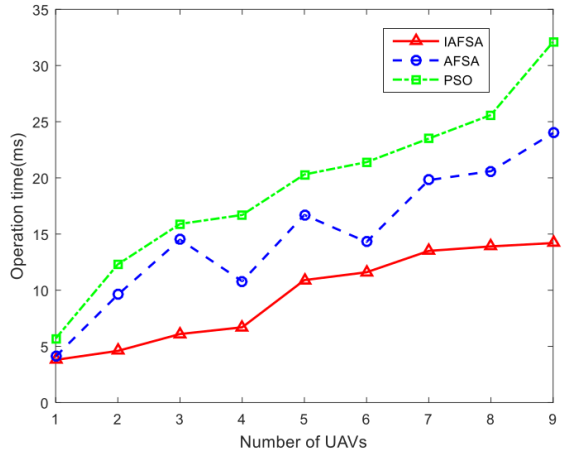

(c) Operation time

Fig. 7. Comparison of experimental results of different numbers of UAVs

success rate of using a single UAV to search for the odor source is less than 30%. However, with the increase in the number of UAV, the success rate of locating the odor source also gradually increases, and the success rate of using the IAFSA to locate the odor source is significantly higher than the AFSA and particle swarm optimization (PSO). When the number of UAV is 4, the success rate of using the IAFSA to locate the odor source reaches 100%, when using the AFSA and PSO to locate the odor source, the success rate can reach 100% when the number of UAV reaches 7 and 8 respectively. This indicates that the IAFSA has a higher success rate in locating the odor source.

The IAFSA not only improves the success rate, but also ensures the accuracy of locating the odor source. It can be seen from Fig. 7b that the location error of the IAFSA is smaller than that of the AFSA and PSO as a whole. When the number of UAV is greater than 4, the location error is kept within 0.1 m. Figure 7c shows the change in the operation time required to locate the odor source with the increase in the number of UAV. The operation time required by the three algorithms to locate the odor source is on the rise as a whole. When the numbers of UAV are the same, the operation time required to locate the odor source by the IAFSA is lower than the AFSA and PSO, which proves that the IAFSA can locate the odor source faster. By analyzing the experimental results in the CFD simulation concentration field, it can be concluded that the improvement of the AFSA in this study is effective, and the IAFSA can achieve better results in locating the odor source.

3.3.2. Influence of UAV's initial position on odor source location

Five UAVs were set up for experiments with different initial positions. The initial coordinates of the UAVs are shown in Table 1. Each group of simulation experiments was conducted 200 times, and the experimental results are shown in Fig. 8.

Table 1
Initial coordinates of UAVs

Initial positions of UAVs	Coordinates/m
Position 1	(15, 8), (10, 8), (18, 5), (12, 2), (11, 11)
Position 2	(16, 8), (11, 8), (19, 5), (13, 2), (12, 11)
Position 3	(17, 8), (12, 8), (18, 5), (14, 2), (13, 11)
Position 4	(14, 8), (9, 8), (17, 5), (11, 2), (10, 11)
Position 5	(13, 8), (8, 8), (16, 5), (10, 2), (9, 11)
Position 6	(15, 9), (10, 9), (18, 6), (12, 3), (11, 12)
Position 7	(15, 7), (10, 7), (18, 4), (12, 1), (11, 10)
Position 8	(15, 6), (10, 6), (18, 3), (12, 5), (11, 9)
Position 9	(13, 6), (8, 6), (16, 3), (10, 2), (9, 9)

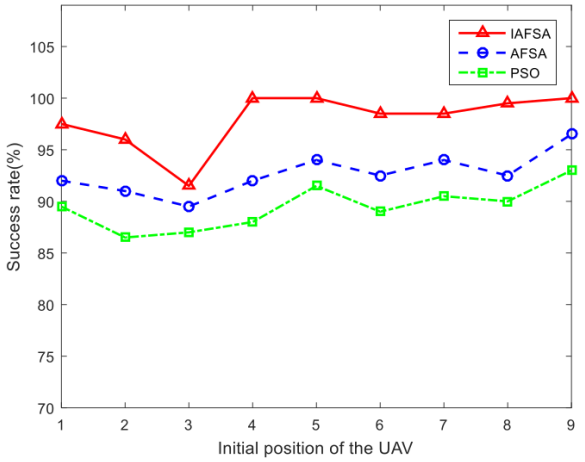

(a) Success rate

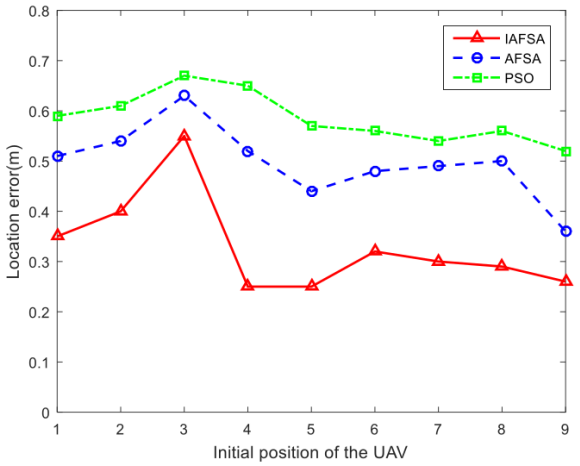

(b) Location error

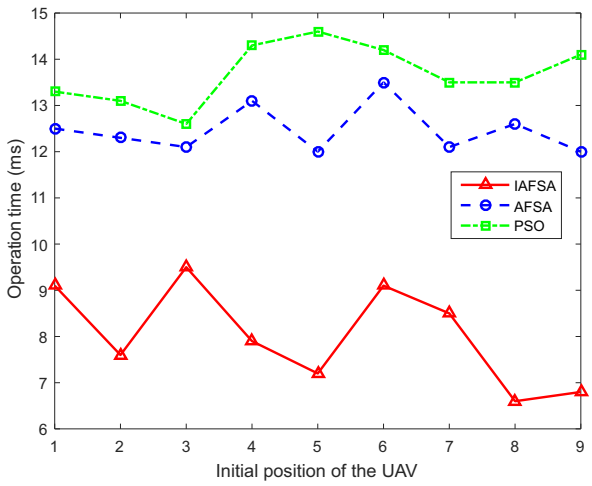

(c) Operation time

Fig. 8. Comparison of experimental results of different initial positions of UAVs

As can be seen in Fig. 8a, in terms of success rate, the success rate of IAFSA is between 91.5% and 100%, the success rate of AFSA is between 89.5% and 96.5%, the success rate of PSO is between 86.5% and 93%, the success rate of IAFSA is always greater than AFSA and PSO. At the same time, it can be seen from Fig. 8a that the success rate of the three algorithms on odor source location does not fluctuate significantly, and the different

initial positions of UAVs have little impact on the success rate of odor source location. In terms of location error, the location error of IAFSA is between 0.25 m and 0.55 m, the location error of AFSA is between 0.36 m and 0.63 m, the location error of PSO is between 0.52 m and 0.67 m, the location error of IAFSA is always smaller than the other two algorithms. At the same time, it can be seen from Fig. 8b that the location error of the three algorithms on odor source location does not fluctuate significantly, and the different initial positions of UAVs have little impact on the location error of odor source location; In terms of operation time, the operation time of IAFSA is between 6.6 ms and 9.5 ms, the operation time of AFSA is between 12 ms and 16.5 ms, the operation time of PSO is between 12.7 ms and 14.6 ms, the operation time of IAFSA is always less than the other two algorithms. At the same time, it can be seen from Fig. 8c that the operation time of the three algorithms on odor source location does not fluctuate significantly, and the different initial positions of UAVs have little impact on the operation time of odor source location.

From the experimental results, no matter the success rate, location error or operation time, the experimental results of the IAFSA are better than the AFSA and PSO. At the same time, different initial positions have little impact on the results of odor source location.

3.3.3. Process of simulation experiments on odor source location

Figure 9 shows the process of five UAVs searching for the odor source in the CFD simulation concentration field. The UAVs search for the odor source with a larger field of vision and step length first, and then after approaching the odor source, the step length is adaptively changed for searching under the regulation of the algorithm. And the field of vision and step length are also increased under the regulation of the algorithm for some UAVs caught in the local peak area, so that they jump out of the local peak area and continue to join the odor source search task.

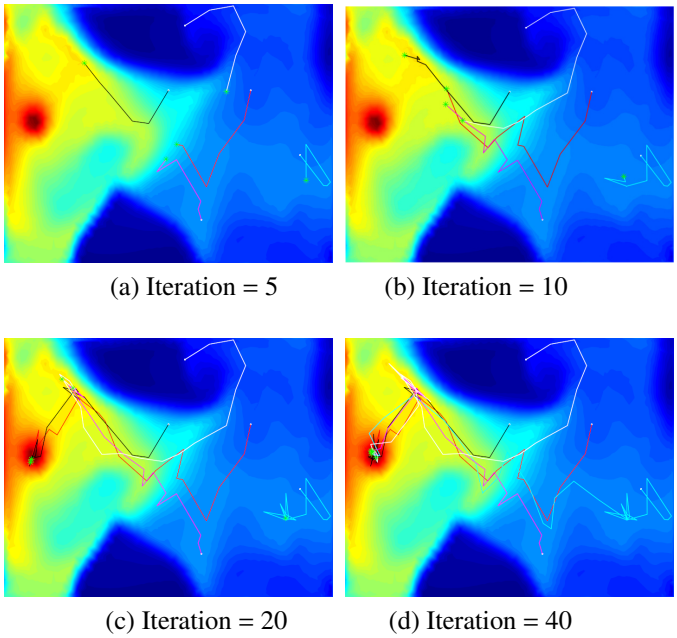

(a) Iteration = 5 (b) Iteration = 10

(c) Iteration = 20 (d) Iteration = 40

Fig. 9. Process of odor source location in CFD simulation concentration field

4. EXPERIMENT ON ODOR SOURCE LOCATION IN SMALL INDOOR SPACES

4.1. Indoor experimental environment construction

Considering that dangerous gases such as methane and carbon monoxide can cause harm to the human body, this study did not choose to use these dangerous gases for experiment when constructing the indoor experimental environment, but chose to use non-toxic, harmless and volatile ethanol to construct an experimental environment. As shown in Fig. 10a, in order to facilitate the volatilization and diffusion of ethanol solution in the room, the ethanol solution with a volume concentration of 75% was loaded into a humidifier in this experiment, so that the ethanol solution was sprayed in the form of a mist, and a small fan with low wind speed was used to assist the volatilization and diffusion of the ethanol solution. As shown in Fig. 10b, due to the limited range of ethanol gas diffusion, as well as other factors such as gas sensors and other restrictions, a small confined space with a length, width and height of 10 m, 10 m and 3 m was chosen as the experimental site for this study.

(a) Odor source (b) Experimental site

Fig. 10. Indoor experimental environment

4.2. Indoor experiment

The initial placement positions of the UAVs and the odor source in the indoor experiment are shown in Fig. 11a. The initial coordinates of the three UAVs are $(1,3.3,0)$, $(1,4.4,0)$ and $(1,5.2,0)$, respectively, and the coordinates of the odor source are $(9,4.4,0.4)$. The flight trajectories of the UAVs when searching for the odor source in the indoor experiment are shown in Fig. 11b, which represents the result of the indoor experiment. According to the search paths in Fig. 11b, each UAV autonomously searched for the odor source and cooperated with each other. When searching for the odor source, UAV 3 fell into the local peak area at a certain moment and hovered around the pseudo-odor source, and then the field of vision and step length of UAV 3 gradually increased through the information sharing among UAVs and the adjustment of the odor source location method, which improved the possibility of UAV 3 to jump out of the local peak area. In this experiment, UAV 3 finally jumped out of the local peak area and successfully located the odor source. It took a total of 26 seconds for the three UAVs

to successfully locate the odor source in this experiment, and the experimental results verified the effectiveness and feasibility of the odor source location method proposed in this study.

(a) Initial positions of the UAVs

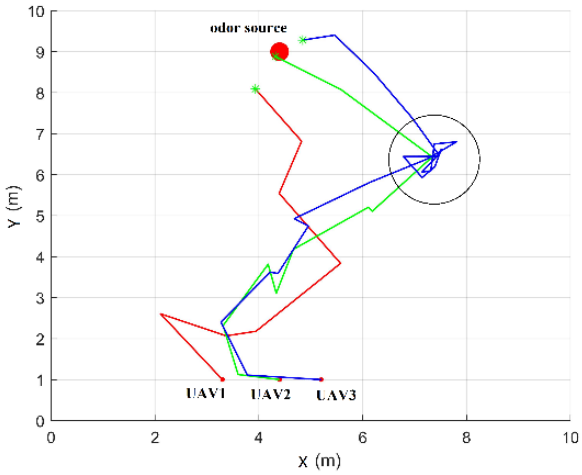

(b) Traceability trajectories of the UAVs

Fig. 11. Indoor experiment

5. CONCLUSIONS

In this study, artificial fish swarm algorithm (AFSA) is applied to the odor source location problem, and the advantages and disadvantages of traditional AFSA in odor source location are analyzed. Combined with the curiosity factor, the field of vision and step length of artificial fish are dynamically adjusted through curiosity, and a multi-unmanned aerial vehicle (UAV) odor source location method based on improved artificial fish swarm algorithm (IAFSA) is proposed. In the simulation experiment, the effect of the number of UAVs on odor source location is first analyzed, and it is proved that when the success rate of odor source location reaches 100%, the number of UAVs required by the IAFSA is less than that required by the basic AFSA and particle swarm optimization (PSO), indicating that the success rate of odor source location by using the IAFSA is higher. And when the number of UAVs is greater than 4, the location error of the IAFSA can be kept within 0.1 m. Then, the effect of the initial positions of the UAVs on the odor source location is analyzed. According to the experimental results, under the conditions of nine different initial positions of the UAVs, the success rate of the IAFSA is maintained between 91.5% and 100%, which is always higher than that of the AFSA and PSO, and the location error of the IAFSA is kept between 0.25 m and 0.55 m. In the indoor traceability experiment, after the UAV fell into the local peak area, the field of vision and step length of the UAV were increased to a certain extent through the adjustment of the IAFSA, so that the UAV jumped out of the local peak area in a short time, which verifies the feasibility and high efficiency of the algorithm, and shows that the multi-UAV odor source location method based on the IAFSA is able to accurately and efficiently complete the odor source location task.

ACKNOWLEDGEMENTS

This study was supported by Zhejiang Provincial Administration for Market Regulation "Young Eagle Plan" cultivation project (No. CY2023003), Zhejiang Provincial Administration for Market Regulation (No. 2022MK058).

REFERENCES

[1] K. Langer, "A guide to sensor design for land mine detection," in *EUREL International Conference The Detection of Abandoned Land Mines: A Humanitarian Imperative Seeking a Technical Solution (Conf. Publ. No. 431)*, 1996, pp. 30–32, doi: 10.1049/cp:19961073.

[2] S.S. Bakhder, G. Aldabbagh, N. Dimitriou, S. Alkhuraiji, M. Fadel, and H. Bakhsh, "IoT networks for monitoring and detection of leakage in pipelines," *Int. J. Sensor Netw.*, vol. 38, no. 4, pp. 241–253, 2022, doi: 10.1504/ijsnet.2022.122559.

[3] M. Hutchinson, H. Oh, and W.H. Chen, "A review of source term estimation methods for atmospheric dispersion events using static or mobile sensors," *Inf. Fusion*, vol. 36, pp. 130–148, 2017, doi: 10.1016/j.inffus.2016.11.010.

[4] Y. Liu, X. Zhao, J. Xu, S. Zhu, and D. Su, "Rapid location technology of odor sources by multi-UAV," *J. Field Robotics*, vol. 39, no. 5, pp. 600–616, 2022, doi: 10.1002/rob.22066.

[5] J. Monroy, J.R. Ruiz-Sarmiento, F.A. Moreno, F. Melendez-Fernandez, C. Galindo, and J. Gonzalez-Jimenez, "A semantic-based gas source localization with a mobile robot combining vision and chemical sensing," *Sensors*, vol. 18, no. 12, p. 4174, 2018, doi: 10.3390/s18124174.

[6] Q. Feng, H. Cai, Y. Yang, J. Xu, M. Jiang, F. Li, and C. Yan, "An experimental and numerical study on a multi-robot source localization method independent of airflow information in dynamic indoor environments," *Sustain. Cities Soc.*, vol. 53, p. 101897, 2020, doi: 10.1016/j.scs.2019.101897.

[7] K. Gaurav, A. Kumar, and R. Singh, "Single and multiple odor source localization using hybrid nature-inspired algorithm," *Sādhanā*, vol. 45, pp. 1–19, 2020, doi: 10.1007/s12046-020-1318-3.

[8] M. Geier, O.J. Bosch, and J. Boeckh, "Influence of odour plume structure on upwind flight of mosquitoes towards hosts," *J. Biol.*, vol. 202, no. 12, pp. 1639–1648, 1999, doi: 10.1242/jeb.202.12.1639.

[9] P. Pyk *et al.*, "An artificial moth: Chemical source localization using a robot based neuronal model of moth optomotor anemo-

tactic search," *Auton. Robot.*, vol. 20, pp. 197–213, 2006, doi: 10.1007/s10514-006-7101-4.

[10] S. Zhang and D. Xu, "A survey of biologically inspired chemical plume tracking strategies for single robot in 2-d turbulence dominated flow environments," in *2011 IEEE/SICE International Symposium on System Integration (SII)*, 2011, pp. 348–353, doi: 10.1109/sii.2011.6147472.

[11] W. Li, J.A. Farrell, and R.T. Card, "Tracking of fluid-advected odor plumes: strategies inspired by insect orientation to pheromone," *Adapt. Behav.*, vol. 9, no. 3–4, pp. 143–170, 2001, doi: 10.1177/10597123010093003.

[12] R.A. Russell, D. Thiel, R. Deveza, and A. Mackay-Sim, "A robotic system to locate hazardous chemical leaks," in *Proceedings of 1995 IEEE International Conference on Robotics and Automation*, 1995, pp. 556–561, doi: 10.1109/robot.1995.525342.

[13] M. Vergassola, E. Villermaux, and B.I. Shraiman, "'Infotaxis' as a strategy for searching without gradients," *Nature*, vol. 445, no. 7126, pp. 406–409, 2007, doi: 10.1038/nature05464.

[14] W. Li, J.A. Farrell, S. Pang, and R.M. Arrieta, "Moth-inspired chemical plume tracing on an autonomous underwater vehicle," *IEEE Trans. on Robot.*, vol. 22, no. 2, pp. 292–307, 2006, doi: 10.1109/tro.2006.870627.

[15] A.J. Lilienthal, M. Reggente, M. Trincavelli, J.L. Blanco, and J. Gonzalez, "A statistical approach to gas distribution modelling with mobile robots-the kernel dm+ v algorithm," in *2009 IEEE/RSJ International Conference on Intelligent Robots and Systems*, 2009, pp. 570–576, doi: 10.1109/iros.2009.5354304.

[16] O. Alvear, N.R. Zema, E. Natalizio, and C.T. Calafate, "Using UAV-based systems to monitor air pollution in areas with poor accessibility," *J. Adv.Transp.*, vol. 2017, p. 8204353, 2017, doi: 10.1155/2017/8204353.

[17] G. Ferri, E. Caselli, V. Mattoli, A. Mondini, B. Mazzolai, and P. Dario, "Explorative particle swarm optimization method for gas/odor source localization in an indoor environment with no strong airflow," in *2007 IEEE International Conference on Robotics and Biomimetics (ROBIO)*, 2007, pp. 841–846, doi: 10.1109/robio.2007.4522272.

[18] Q.H. Meng, W.X. Yang, Y. Wang, and M. Zeng, "Multi-robot odor-plume tracing in indoor natural airflow environments using an improved ACO algorithm," in *2010 IEEE International Conference on Robotics and Biomimetics*, 2010, pp. 110–115, doi: 10.1109/robio.2010.5723312.

[19] D. Zarzhitsky, D. Spears, D. Thayer, and W. Spears, "Agent-based chemical plume tracing using fluid dynamics," in *International Workshop on Formal Approaches to Agent-Based Systems*, 2004, pp. 146–160, doi: 10.1007/978-3-540-30960-4_10.

[20] D. Zarzhitsky, and D.F. Spears, "Swarm approach to chemical source localization," in *2005 IEEE International Conference on Systems, Man and Cybernetics*, 2005, vol. 2, pp. 1435–1440, doi: 10.1109/icsmc.2005.1571348.

[21] Z. Zhao and J. Fang, "Robot odor localization based on evolutionary gradient algorithm under the Gaussian plume model," in *Future Information Engineering and Manufacturing Science*, 2015, pp. 337–342, doi: 10.1201/b18167-72.

[22] F. Pourpanah, R. Wang, C.P. Lim, X.Z. Wang, and D. Yazdani, "A review of artificial fish swarm algorithms: Recent advances and applications," *Artif. Intell. Rev.*, vol. 56, no. 3, pp. 1867–1903, 2023, doi: 10.1007/s10462-022-10214-4.

[23] M. Pantusheva, R. Mitkov, P.O. Hristov, and D. Petrova-Antonova, "Air Pollution Dispersion Modelling in Urban Environment Using CFD: A Systematic Review," *Atmosphere*, vol. 13, no. 10, p. 1640, 2022, doi: 10.3390/atmos13101640.